

# DESIGN CHOICES FOR THE CRYOGENIC CURRENT COMPARATOR FOR FAIR\*

T. Sieber<sup>†</sup>, H. Braeuning, M. Schwickert, GSI, Darmstadt, Germany  
 L. Crescimbeni<sup>1</sup>, F. Schmidl, Friedrich-Schiller-University Jena, Jena, Germany  
 R. Stolz<sup>3</sup>, M. Schmelz<sup>3</sup>, V. Zakosarenko<sup>4</sup>, Leibniz IPHT, Jena, Germany  
 T. Stoehlker<sup>1,2</sup>, V. Tympel<sup>1</sup>, Helmholtz Institute Jena, Jena, Germany  
 J. Tan, G. Khatri, T. Koettig, CERN European Organization for Nuclear Research, Geneva, Switzerland

<sup>1</sup>also at GSI Helmholtz Centre for Heavy Ion Research, Darmstadt, Germany

<sup>2</sup>also at Institute for Optics and Quantum Electronics, Jena, Germany

<sup>3</sup>also at Technical University Ilmenau, Ilmenau, Germany

<sup>4</sup>also at supracon AG, Jena, Germany

## Abstract

The Cryogenic Current Comparator (CCC) is a superconducting SQUID-based device, which measures extremely low electrical currents via their azimuthal magnetic field. Triggered by the need for nA current measurement of slow extracted beams and weak beams of exotic ions in the storage rings at FAIR and CERN, the idea of the CCC as a diagnostics instrument has been revitalized during the last ten years. The work of a collaboration of institutes specialized on the various subtopics resulted in a large variety of CCC types with respect to field-pickup, magnetic shielding, SQUID types and SQUID coupling. Many of them have been tested under laboratory and under beamline conditions, which formed a detailed picture of the application possibilities for CCCs in accelerators.

In parallel to CCC detector development the cryogenic support system has steadily been optimized, to fulfil the requirement of a standalone liquid helium cryostat, which is nonmagnetic, fit for UHV application, vibration damped, compact and accessible for maintenance and repair. We present the major development steps of the CCC for FAIR. The latest beamtime results are shown as well as recent tests with the cryogenic system. The most promising CCC type for FAIR is the so called Dual-Core CCC (DCCC), which runs two pickups in parallel with independent electronics for noise reduction. The magnetic shielding has an axial meander geometry, which provides superior attenuation of external magnetic noise.

## INTRODUCTION

The CCC measures the beam intensity via the beam azimuthal magnetic field, which is for nA currents in the fT range. It consists of a superconducting shielding, which provides an attenuation of non-azimuthal external fields in the range -70 dB to -140 dB, depending on the shield geometry. The shielding guides the superconducting Meissner-Current, generated by the beam magnetic field, to an internal pickup loop. The pickup loop is a coil with

only one winding around a high permeability ring core, which acts as a flux concentrator. The ring core is used in the ‘classical’ CCC as shown in Fig. 1 to provide an efficient coupling of the magnetic field to the SQUID circuit. The arrangement is a transformer with the particle beam as primary winding and the pickup coil as the secondary winding. The signal from the pickup coil is fed via an additional matching transformer for impedance matching to a DC SQUID (Superconducting Quantum Interference Device) magnetometer. For current calibration of the system, a second coil is added. Figure 1 shows the classical CCC arrangement, originally developed at the PTB (Physikalisch-Technische Bundesanstalt) [1] and adapted to the accelerator application at GSI [2].

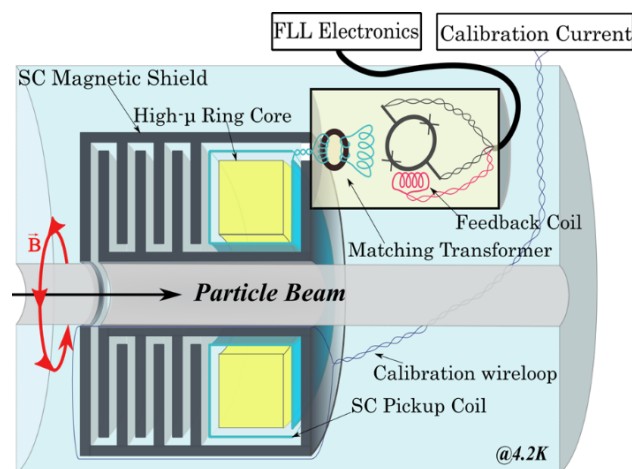


Figure 1: Classical CCC, shielding geometry with radial meanders and high permeability ring core.

The SQUID is operated in a compensation circuit, using a so called Flux Locked Loop (FLL) electronics [3, 4], which generates via a feedback system a compensation field to the beam magnetic field. If the working point of the FLL system is locked to the steepest slope of the flux/voltage curve of the SQUID, the resolution can be in the order of  $\mu\Phi_0$  ( $\Phi_0$ =magnetic flux quantum). Figure 2 shows a schematic of the electronics and the working point in the flux/voltage curve.

\* Work supported by BMBF under contracts 05P18RDRB1 and 05P18SJR B1.

<sup>†</sup>T.Sieber@gsi.de

Investigations at IPHT Jena have shown that it is possible to build a CCC with an axial meander geometry [5], consequently the development is called axial CCC, see Fig. 3, middle. This shielding/pickup design provides a several orders of magnitude higher attenuation of external magnetic disturbances due to the increased meander path length. So far the coreless axial CCC could not be operated in the CCC cryostat due to its weak coupling to beam current (resp. calibration current) and its sensitivity to external noise [6].

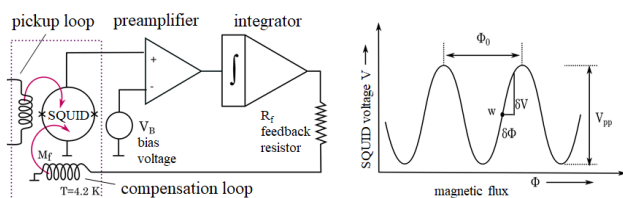


Figure 2: Left: schematic of the FLL electronics. Right: SQUID characteristic flux/voltage curve,  $W$  marks the working point. The Oscillation period is one flux quantum  $\Phi_0 = h/2e = 2.07 \times 10^{-5} \text{ Tm}^2$ .

A third CCC type has been developed to connect the axial meander geometry with a doubled classical toroidal core pickup [7, 8]. This version, called the Dual Core CCC or DCCC, combines the positive features of the two earlier types. Figure 3 shows the three CCC varieties at one glance. The DCCC is our preferred candidate for FAIR. Beam tests with slow extracted beams from SIS18 synchrotron have recently been performed.

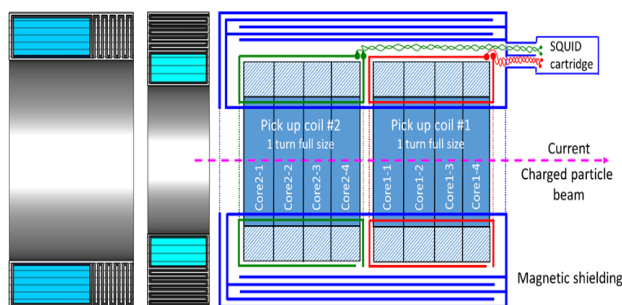


Figure 3: Magnetic shieldings with radial (left) and axial (middle) meanders. The ring-core of the radial CCC is indicated in blue, the detector volume of the axial CCC in turquoise. Right: Schematic sectional view of the DCCC with axial meanders and two independent, fourfold segmented (due to material width limitations) toroidal cores.

## BEAM TESTS WITH DUAL-CORE CCC

The DCCC was originally designed to eliminate the low frequency disturbances from magnetization jumps, which have been observed in the Nanoperm<sup>®</sup> toroidal cores. Since these jumps occur randomly in each core, they can easily be subtracted from the beam current signal (seen by both pickups/cores simultaneously), which leads to an improved SNR. To match the requirements of the FAIR 150 mm beamline and to fit into the cryostat of the FAIR CCC-XD

[9, 10]. Our DCCC prototype for beam tests was designed to a length of 200 mm, an inner diameter of 250 mm, outer diameter 350 mm. The lead structure has a weight of 39 kg. The magnetic shielding comprises 7 axial meander pairs, each with a total path length of 140 cm. The resulting attenuation of non-azimuthal magnetic fields was determined by Helmholtz coil measurement to  $< -140 \text{ dB}$  (compared to  $-70 \text{ dB}$  with the radial meander shielding).

The DCCC was installed in an experimental cave at SIS18 synchrotron. Our goal was 1. to investigate and demonstrate the current resolution and bandwidth (and slew rate limitations) of the system, 2. to show its capability to analyze effects of spill optimization processes and serve as detector for corresponding feedback system. Figure 4 shows a photo of the experimental setup.



Figure 4: CCC cryostat during LN filling. The system is installed in an experimental cave at the SIS18 beamline.

In a first campaign we used a 400 MeV/u Erbium 57+ beam with a nominal intensity of  $5 \times 10^8$  particles per spill, later we switched to a 400 MeV/u Ar 18+ beam with  $2 \times 10^9$  particles per spill. Already without beam it was obvious, that the noise behavior of the two SQUIDS of the DCCC was not identical, which is a result of individual material differences and non-symmetric setup - mainly different orientation of the pickup coils with respect to noise sources and different cable lengths between SQUIDS and pickup coils. Figure 5 shows the twofold noise spectrum of the DCCC. The two pickups/SQUIDS are named due to the color of their cables in “red” and “yellow”. Remarkably the SQUID with worse noise behavior showed a higher slew rate, means higher stability at fast current changes, an aspect which is currently under discussion.

The SIS18 spills had nominal lengths between 100 ms and 1 s. Since the Erbium intensity was quite low, preferably short spills were used to reach reasonable intensities. Figure 6 shows a 30 ms spill at a current of 300 nA with liquefier noise filtered and unfiltered. The general noise floor was in the range of 10 nA for the yellow SQUID and

doubled for the red SQUID, while the 8.4 Hz noise (6<sup>th</sup> harmonic of the 1.4 Hz liquefier pulse) could even reach 150 nA for the red SQUID. While the white noise is random, the main (periodic) perturbation at 8.4 Hz and 30 Hz could be filtered out. The strongest perturbation (8.4 Hz) occurred due to mechanical coupling between liquefier and detector and could be eliminated mechanically.

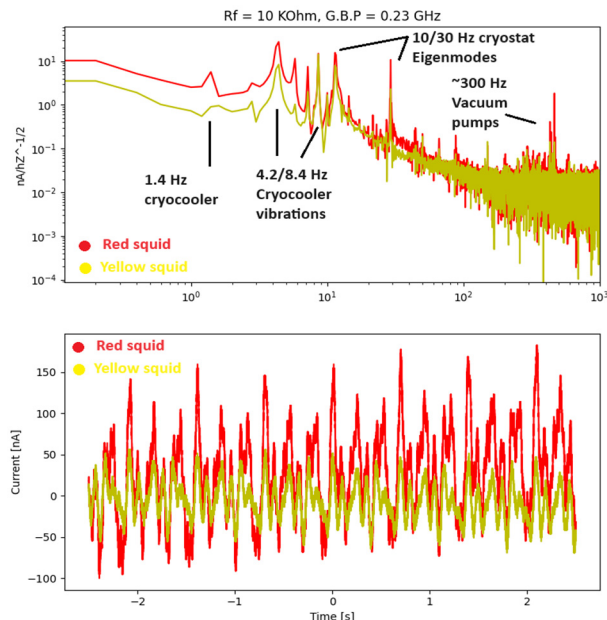


Figure 5: Current noise from the FAIR DCCC prototype, for its two SQUIDs. Upper: FFT with main noise sources highlighted. Lower: Noise in time domain.

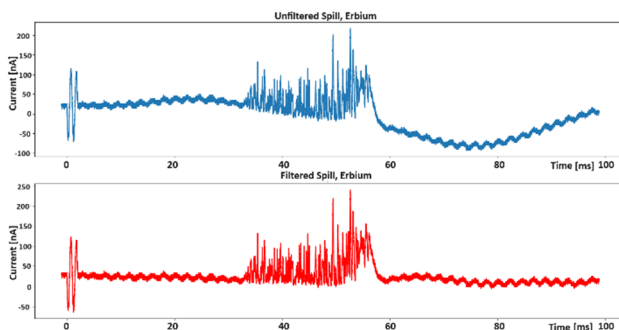


Figure 6: 30 ms spill (Er 57+,  $1 \times 10^8$  particles). Upper: unfiltered, lower: filtered (software), both with 120 nA calibration sine-pulse on the left. As shown here, periodic noise will be filtered in the CCC FESA class without deforming the spill structure.

## SPILL OPTIMIZATION PROCESS

The DCCC could be used for analysis of the spill quality and as a detector for an automatic spill optimization system, which was developed at GSI [11], the latter with some limitation because of slew rate problems and bad spill quality. Figure 7 shows an example for the so called “tune wobbling” technique [12], which is applied to quadrupole driven extraction. A periodic signal is superimposed to the steering voltage of the quadrupole, which drives the particles to betatron resonance. Due to the “wobbling” the

effect of the power supply noise is reduced, which results in a more homogeneous spill structure and therefore higher detector efficiency at the physics experiments.

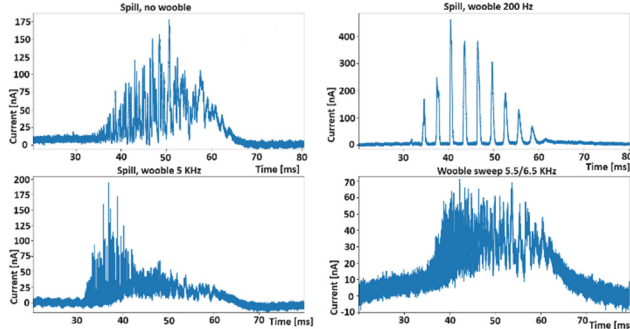


Figure 7: 30 ms spill ( $5 \times 10^8$  Ar 18+ per spill). Top left: uncorrected spill. Top right: 200 Hz wobbling frequency, spill modulation. Bottom left: 5 kHz, spill starts to smoothen out (frequency higher than beam cutoff frequency, around 4 kHz). Bottom right: Optimal setting for spill quality (6 kHz  $\Delta f=500$  Hz).

Obviously the DCCC worked very well for online analysis and optimization of tune wobbling parameters, providing at the same time a calibrated nA intensity measurement. However, when we switched to KO extracted beams and tried to integrate the CCC into the automatized GNU radio feedback system, we found excessive background noise and encountered severe slew rate problems at higher intensities. The latter resulted in frequent “flux jumps” when the FLL electronics lost its working point (illustrated in Fig. 2). We concluded that at this extraction scheme some spikes were too fast and/or too high for the electronics feedback loop and finally caused the jumps. Figure 8 shows an example for a measurement interrupted by a flux jump. After a few ms the CCC jumps to an arbitrary working point. The current calibration is still valid, so the spill could in principle be re-constructed.

The maximum slew rate of our system from laboratory measurements is  $0.4 \mu\text{A}/\mu\text{s}$ . Although the measured spikes were below this limit and although we could not find higher frequency components in the FFT, we assume that there are faster spikes at the moment of breakdown. As a next step we will reduce the noise in our experimental setup and investigate if there is a general limitation for CCC at KO extraction, or if the problems occurred from extraction settings at this particular campaign.

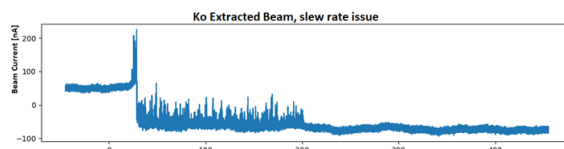


Figure 8: Flux jump due to exceeded slew rate.

## CRYOGENIC SYSTEM OPTIMIZATION

The CCC needs a complex dedicated cryogenic support system. The cryostat itself has steadily been optimized, to fulfil the requirement of a standalone liquid helium cryostat, which is nonmagnetic, fit for UHV application,

vibration damped, compact and accessible for maintenance and repair. Figure 9 shows schematically the FAIR prototype cryostat, it basically consists of a LHe container covered by a thermal shield, which is cooled to  $\sim 90\text{K}$  by the evaporated Helium gas. The isolation vacuum chamber is a stainless steel frame with Al windows which allow reasonably good access to the inner structure and the CCC [13]. The attached reliquefier is of the type Cryomech HeRL10 with a liquefaction rate of 15 l/day. During our previous campaigns we realized that the cooling power of this liquefier type is too low to allow for self-sufficient standalone operation. Operation time was limited to max. 10 days, therefore we switched to a 25 l/day system, which is firstly tested at the time of this report.

It should also be mentioned here, that in parallel to a cooling scheme with a He bath cryostat investigations are ongoing at CERN to cool the CCC with a semi-dry cryostat, to simplify (and downsize) the setup and to avoid disturbances by He boil-off [14].

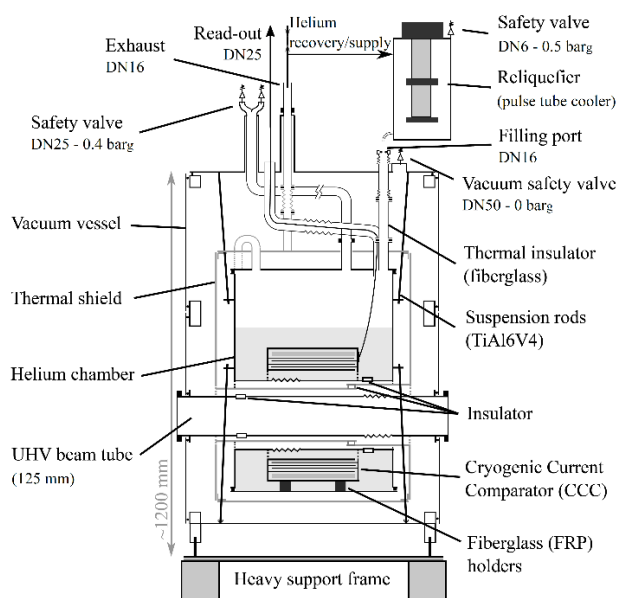


Figure 9: Cryostat of the FAIR CCC-XD, which was used for our beam tests with the DCCC. Size: 1.2 m  $\times$  0.8 m  $\times$  0.8 m. The LHe container is suspended by Ti wires and surrounded by an enthalpy cooled copper shield.

## SUMMARY AND OUTLOOK

A new dual core type DCCC has been tested in the laboratory and in the beamline. It showed excellent magnetic shielding properties and proved the possibility of noise reduction by combination of two SQUID signals. The costs of a Pb DCCC are around 1/10 of a Niobium system. Some optimization work is required to improve the performance, as one important step, the DCCC will be designed to have a more symmetric layout, the observed slew rate problems will (if persistent) be solved by using matching transformers like for the CCC-XD. We consider the DCCC as the most promising candidate for CCC at FAIR. Concerning controls, a FESA class has been

developed and could be tested during our beamtime, including filtering of periodic noise.

After extensive tests of our cryostat we expect to reach the required stand-alone operation for the FAIR tunnels by switching to a more powerful re-liquefier with a liquefaction rate of 25 l/day, test of the system is ongoing.

## REFERENCES

- [1] K. Grohmann *et al.*, "Field attenuation as the underlying principle of cryocurrent comparators 2. Ring cavity elements", *Cryogenics*, vol. 16, pp. 601-605, 1976. doi:10.1016/0011-2275(76)90192-2
- [2] A. Peters *et al.*, "A Cryogenic Current Comparator for the absolute Measurement of nA Beams", *AIP Conf. Proc.*, Stanford, California USA, May 1998, pp. 163-180. doi:10.1063/1.56997
- [3] F. Kurian, "Cryogenic Current Comparators for precise Ion Beam Current Measurements", Ph.D. thesis, University of Frankfurt, Germany, 2015.
- [4] <http://www.magnicon.com/squid-electronics>
- [5] V. Zakosarenko *et al.*, "Coreless SQUID-based cryogenic current comparator for non-destructive intensity diagnostics of charged particle beams", *Supercond. Sci. Technol.*, vol. 32, pp. 014002, 2018. doi: 10.1088/1361-6668/aaf206
- [6] L. Crescimbeni *et al.*, "Axial Cryogenic Current Comparator (CCC) for FAIR", in *Proc. IBIC'23*, Saskatoon, Canada, Sep. 2023, pp. 259-262. doi:10.18429/JACoW-IBIC2023-TUP034
- [7] V. Tympel *et al.*, "Creation of the First High-Inductance Sensor of the New CCC-Sm Series", in *Proc. IBIC'22*, Kraków, Poland, Sep. 2022, pp. 469-472. doi:10.18429/JACoW-IBIC2022-WEP30
- [8] M. Stapelfeld, "Experimentelle Untersuchungen zum Systemdesign von Kryogenen Stromkomparatoren", Ph.D. thesis, Friedrich Schiller University Jena, Germany, 2022.
- [9] V. Tympel *et al.*, "Cryogenic Current Comparators for 150 mm Beamline Diameter", in *Proc. IBIC'17*, Grand Rapids, MI, USA, Aug. 2017, pp. 431-434. doi:10.18429/JACoW-IBIC2017-WEPFC07
- [10] T. Sieber *et al.*, "Optimization Studies for an Advanced Cryogenic Current Comparator (CCC) System for FAIR", in *Proc. IBIC'16*, Barcelona, Spain, Sep. 2016, pp. 715-718. doi:10.18429/JACoW-IBIC2016-WEPG40
- [11] P. J. Niedermayer *et al.*, "Software-Defined Radio Based Feedback System for Beam Spill Control in Particle Accelerators", in *Proc. GRCon23*, Tempe, Arizona, USA, 2023. <https://pubs.gnuradio.org/index.php/grcon/article/view/133>
- [12] R. Singh, P. Forck and S. Sorge, "Reducing Fluctuation in Slow Extraction Beam Spill using Transit-Time-dependent Tune Modulation", *Phys. Rev. Applied* 13, 044076, April 2020. doi:10.1103/PhysRevApplied.13
- [13] D. M. Haider, "Precise Intensity Monitoring at CRYRING@ESR: On designing a Cryogenic Current Comparator for FAIR", Ph.D thesis, Institute for Applied Physics, IAP, University of Frankfurt, 2023.

- [14] A. Onufrena *et al.*, “Remote cooling systems with mesh-based heat exchangers for cryogenic applications”, *IOP Conf. Ser.: Mater. Sci. Eng.* vol. 1240, p. 012049, 2022.  
doi:10.1088/1757-899X/1240/1/012049